



# Spontaneous Collapse Mechanism of World Trade Center Twin Towers and Progressive Collapse in General

Jia-Liang Le, M.ASCE<sup>1</sup>; and Zdeněk P. Bažant, Hon.M.ASCE<sup>2</sup>

**Abstract:** The collapse of the World Trade Center (WTC) Towers during the terrorist attacks on September 11, 2001, remains one of the most tragic catastrophes in the field of structural engineering. This paper first reviews a mathematical model that explains the process of the total collapse of the Twin Towers and shows that the downward collapse progression below the impacted floors was spontaneous. The model is based on a continuum description of the motion of the crush front and captures various types of energy dissipation during the collapse. The predictions of this model match all the observations, including the video records of the first few seconds of motion of both towers, the seismic records of the collapse durations for both towers, the mass and size distributions of comminuted concrete particles, and the fast expansion of dust clouds during collapse with the booms generated. This catastrophe provoked general interest in other types of progressive collapse of buildings. This is the subject of the second part of this paper, in which a three-dimensional stochastic computational model for the collapse of RC frame buildings is presented. The occurrence probabilities of different collapse patterns are predicted. The model is further extended to investigate the delayed collapse behavior of RC frames. The results of the analysis shed light on the emerging trend of probabilistic analysis and design of structures against progressive collapse. DOI: [10.1061/\(ASCE\)ST.1943-541X.0003342](https://doi.org/10.1061/(ASCE)ST.1943-541X.0003342). © 2022 American Society of Civil Engineers.

## Introduction

Research on progressive collapse has a rich history dating back to the 1968 collapse of the Ronan Point apartment building. Over the years, various collapse incidents have stimulated an increasing interest in understanding the mechanism of progressive collapse in the pursuit of improved resilience of civil structures against such a catastrophic failure. The most notable case is the collapse of the World Trade Center (WTC) Twin Towers in New York City, New York, during the terrorist attacks on September 11, 2001, which caused 2,763 human casualties, enormous financial loss, and has had a profound societal impact until today. To the structural engineering community, this tragic collapse raised many new intellectual questions related to the progressive collapse mechanics, which are of both scientific and practical importance.

Over the last two decades, extensive efforts have been devoted to investigating the collapse of the WTC towers. Soon after the collapse, Bažant (2001) and Bažant and Zhou (2002) performed a simple analysis of the collapse initiation, and soon afterward, Kausel (2001) published a similar simplified analysis. The former analysis also showed that what triggered the fall was the viscoplastic buckling of columns heated for a sufficiently long time, which caused the top part of each tower to fall through at least one story height. The kinetic energy of the upper falling part was immediately (Bažant 2001) shown to be many times greater than the maximum possible energy absorption capacity of the columns of the underlying story, which

made a progressive story-by-story collapse inevitable. This energy analysis provided a simple proof of the spontaneity of the downward progression of collapse of WTC towers triggered by the prolonged simultaneous fire heating of a very large volume after the aircraft impact. The analysis also showed that the aircraft impact could not topple the tower to the side, that right after the impact the rest of the whole structure outside the impacted zone must have remained undamaged and elastic, and that the lateral deflection of the tower caused by the impact was only about 0.4 m.

Various numerical studies were carried out to clarify the details of structural damage due to aircraft impact and elevated temperatures (Quintiere et al. 2002; Abboud et al. 2003; Wierzbicki and Teng 2003). A particularly extensive and comprehensive investigation on the collapse (NIST 2005) was performed by the National Institute of Standards and Technology (NIST). It involved experimental investigation of the damaged pieces of trusses and columns, as well as a high-fidelity numerical simulation of the fire-induced structural damage and the overall response of the impacted floors to the damage. Although this analysis did not deal with the progressive collapse of the towers, it did clarify the important factors that eventually initiated the collapse with a roughly hour-long delay after the impact. It revealed the extent of immediate damage caused directly by aircraft impact, clarified the mechanical behavior of load-bearing structural components during the fire and, importantly, provided photographic documentation of large buckling deflections of exterior columns exposed to fire for a long time.

For the collapse, the crucial difference from previous fires in tall buildings was that this fire was ignited simultaneously over a large volume of several stories. This caused the surface-to-volume ratio of the fire zone to be much smaller than in previous fires, which reduced the cooling rate and thus led to higher temperatures (normally the fire moves—when a neighboring place starts burning, the previous one is already cooling).

NIST's analysis supports Bažant and Zhou's (2002) conclusion that as soon as the top part of each tower fell through the height of at least one story, the whole tower was doomed to suffer a total collapse (NIST 2005). The NIST, however, did not attempt to

<sup>1</sup>Professor, Dept. of Civil, Environmental, and Geo-Engineering, Univ. of Minnesota, Minneapolis, MN 55455. ORCID: <https://orcid.org/0000-0002-9494-666X>

<sup>2</sup>McCormick Institute Professor and W. P. Murphy Professor of Civil and Mechanical Engineering and Materials Science, Northwestern Univ., Evanston, IL 60208 (corresponding author). Email: z-bazant@northwestern.edu

Note. This manuscript was submitted on September 28, 2021; approved on January 24, 2022; published online on April 8, 2022. Discussion period open until September 8, 2022; separate discussions must be submitted for individual papers. This paper is part of the *Journal of Structural Engineering*, © ASCE, ISSN 0733-9445.

model the triggering of dynamic collapse and its downward progression. Many observations, such as the total collapse duration, high speed ejection of debris and air with loud booms, the origin of very fine concrete particles and dust, were not analyzed by NIST. Of course, a detailed numerical modeling of the entire collapse process, with finite-element discretization of all columns and floors and gas flows, would have been computationally infeasible. But such a brute-force approach has actually been shown unnecessary.

The fact that the stories were numerous and that the collapse was vertical and almost simultaneous over the full tower width made possible a simplified, although realistic, one-dimensional (1D) continuum analysis. A 1D continuum model for the vertical collapse propagation of the crush front was developed by Bažant and Verdure (2007). They applied d'Alembert's principle to formulate the dynamic equilibrium of the upper falling part, and then to derive the equations for the crush-down and crush-up phases of the collapse process.

In the subsequent studies, the model was further refined by incorporating different energy dissipation sources, such as the impact comminution of concrete slabs, fast ejection of air, and lateral ejection of debris (Bažant et al. 2008; Le and Bažant 2011, 2017a). The model was shown to match all the observations, which include video records of the motion of the upper falling part during the first few seconds of the collapse (before dust clouds obscured the view), the total collapse duration inferred from the seismic record, the particle-size distributions of the dynamically comminuted concrete floors, the explosive expansion of dust clouds, and the booms heard. This analysis dispelled all the main claims of the proponents of the controlled demolition hypothesis, which include the free-fall motion of the tower, pulverization of concrete slabs by explosives, wide spreading of concrete particles, and dust burst and booms supposedly due to explosions. The analysis showed them all to be false.

Beyond clarifying what did and did not cause the whole WTC towers to collapse, the analysis of this catastrophe also provoked a continued effort to develop advanced experimental techniques and numerical tools for the mechanics of progressive collapse, with a focus on typical reinforced concrete (RC) and steel structures. Significant advances have been made. Several successful collapse experiments have been performed on the structural subassemblages subjected to local column removal (Lew et al. 2011; Sadek et al. 2011; Xiao et al. 2015). Although these experiments were limited to substructural and reduced-scale structural systems, they revealed some essential structural behaviors under large deformations during the collapse process. Meanwhile, several investigators studied the collapse resistance of some existing full-scale buildings (Sasani and Sagioglu 2008; Sasani et al. 2011; Song and Sezen 2013).

Due to the prohibitive cost of full-scale collapse experiments, numerical simulations have become the major tool for studying progressive collapses (El-Tawil et al. 2014; Kiakojoouri et al. 2020). The recent numerical modeling included continuum finite-element simulations (Alashker et al. 2011), discrete element-based models (Masoero et al. 2010), and macroelement-based reduced-order models (Kaewkulchai and Williamson 2004; Khandelwal and El-Tawil 2008; Bao et al. 2008). These models were capable of capturing various essential deformation and damage mechanisms of structural components during the collapse process, such as material damage, catenary action, membrane action, Vierendeel frame action, and debris impact. The advances in computational modeling opened further opportunities for reliability-based analysis and design of buildings against progressive collapse, which has been an important line in recent research (Ellingwood 2006; Ellingwood et al. 2007; Xu and Ellingwood 2011; El-Tawil et al. 2014).

In recent studies (Le and Xue 2014; Xue and Le 2016c, b), a two-scale stochastic computational model was proposed to calculate the progressive collapse risk of RC buildings. It was shown that, depending on the random loads and material properties, structures could exhibit different collapse patterns and degrees of failure. The new model was also able to quantify the occurrence probabilities of different collapse patterns.

This first part of this paper provides a succinct review of the 1D mathematical model for the collapse progress of the WTC towers. The second part of the paper is devoted to a recently developed two-scale numerical model for stochastic analysis of general RC frame structures, with an effort toward probabilistic assessment and design of structures against progressive collapse.

## Mathematical Model of WTC Collapse

The collapse of WTC towers is a very complex process involving numerous nonlinear and random phenomena with only fragmentary information, and so a direct and detailed numerical simulation is not feasible. The detailed computational simulation of NIST could not have been extended beyond the few impacted stories under fire.

Nevertheless, for the purpose of basic understanding of the overall collapse behavior, it is not necessary to explicitly model every individual phenomenon. Instead, it suffices to capture realistically the essential dynamics of motion with the major energy dissipation mechanisms. To develop a tractable mathematical model, two important features of the WTC collapse should be noted: (1) at collapse initiation, the crush front formed across the whole width of tower and continued as such all the way down, which meant that during the entire collapse process, the motion of the crush front can be idealized as one-dimensional; and (2) due to the height of the WTC towers, the crush front moved through numerous floors, and therefore it is legitimate to model the movement of the crush front using a continuum framework.

Based on these considerations, a 1D continuum model was developed to describe the motion of the crush front (Bažant and Verdure 2007; Bažant et al. 2008; Le and Bažant 2017a). This appears to be so far the only model that captures the entire collapse process, and also matches all the observations including (1) the video record of the initial falling motion of the tower, (2) the exact recorded collapse duration, (3) the observed fragment-size distribution of the dynamically comminuted concrete slabs, (4) the explosivelike ejection of air and debris, and (5) the loud booms heard during the collapse.

### Model Formulation

Fig. 1 presents a schematic of the entire collapse process. Scenes I–III show the process of structural damage caused by the aircraft impact and fire. As the columns on the impacted floors lose their load resistance, the crush front forms and the collapse initiates. The details of the damage of the impacted floors and the formation of the crush front have been given by NIST (2005). Once the collapse initiates, the crush front propagates downward and crushes the lower part of the tower, shown by Scene IV of Fig. 1. This is referred to as the crush-down phase. As the entire lower part of the tower gets crushed, the upper falling part hits on the compacted debris resting on the ground with a large velocity, and is crushed at the bottom by the debris (Scene V). This causes the crush front to propagate upward throughout the falling upper intact part of the tower (Scene VI). This is referred to as the crush-up phase.

In the simplified 1D model (Bažant and Verdure 2007; Bažant et al. 2008; Le and Bažant 2017a), the tower is considered as a 1D continuum of mass density  $\mu(z)$  distributed along the height, where

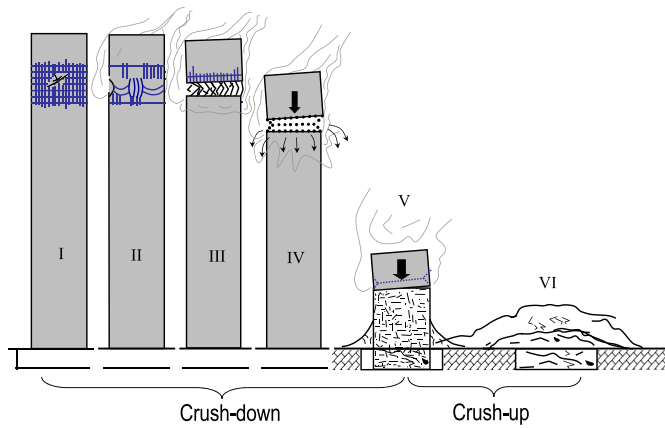


Fig. 1. Schematic of the collapse process of WTC towers.

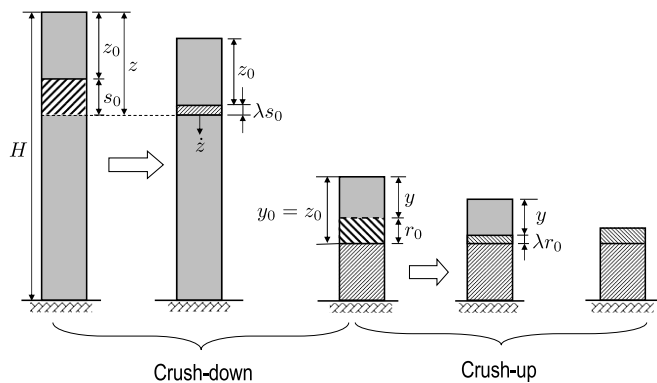


Fig. 2. Mathematical modeling of crush-down and crush-up phases.

$z$  denotes the distance of the current position of the crush front from the initial position of the tower top (Fig. 2). The total mass of the upper falling part is  $m(z) = \int_0^z \mu(\zeta) d\zeta$ .

As the lower part of the tower is getting crushed, the material is getting compressed to a higher density  $\mu_c$ . Meanwhile, during the crushing process, a fraction, denoted by  $\kappa_0$ , of the mass is ejected out of the tower. An initially intact layer of height  $s_0$  is crushed into a compacted layer of height  $\lambda s_0$ , where  $\lambda =$  compaction ratio  $= (1 - \kappa_0)\mu/\mu_c$ . The crushing process is idealized to be concentrated at the crush front, which propagates at velocity  $\dot{z} = dz/dt$ . During a time interval  $\Delta t$ , an intact layer of height  $\dot{z}\Delta t$  gets crushed to a layer of height  $\lambda\dot{z}\Delta t$ . Therefore, the upper falling part moves down by a distance of  $(1 - \lambda)\dot{z}\Delta t$ , and its downward velocity is  $(1 - \lambda)\dot{z}$ .

Based on the foregoing discussion, the momentum of the upper falling part is  $[1 - \lambda(z)]m(z)\dot{z}$ . The motion of the falling part is driven by its gravity  $m(z)g$ , where  $g$  is gravity acceleration  $= 9.81 \text{ kg} \cdot \text{m/s}^2$ , but meanwhile is resisted by a force  $F_c$ , which is derived from all the major energy dissipations during the destruction process. By using the d'Alembert principle, the following differential equation can be written to describe the crush-down phase (Bažant and Verdure 2007; Bažant et al. 2008; Le and Bažant 2017a):

$$\frac{d}{dt} \left\{ [1 - \lambda(z)]m(z) \frac{dz}{dt} \right\} - m(z)g = -F_c(z, \dot{z}) \quad (1)$$

Eq. (1) can also be derived from an extended Lagrangian formulation for dynamic systems involving a moving mass varying as a function of front coordinate  $z$  (Pesce et al. 2012).

One can also perform the same analysis for the crush-up phase, which begins after all the stories below the fire zone got compacted and rest on the ground. The main difference between the crush-down and crush-up phases is that in the crush-up phase, the compacted layer is stationary (Fig. 2). By noting this difference, the motion of the crush front during the crush-up phase can be described by (Bažant and Verdure 2007)

$$m(y) \frac{d}{dt} \left\{ [1 - \lambda(z)] \frac{dy}{dt} \right\} + m(y)g = F_c(y, \dot{y}) \quad (2)$$

where  $y =$  vertical coordinate of the upper boundary of the crushed zone measured from the top of tower in the initial undamaged state (Fig. 2).

What remains to be determined is the effective resisting force  $F_c$ . Arguments were given to calculate it as  $F_c = F_b + F_s + F_a + F_e$ , where  $F_b$ ,  $F_s$ ,  $F_a$ , and  $F_e$  denote the equivalent resisting forces generated by four energy dissipation mechanisms, which include (1) buckling and fracture of the steel columns ( $F_b$ ), (2) comminution of concrete slabs ( $F_s$ ), (3) air ejection around the building perimeter at speeds high enough to create sonic booms ( $F_a$ ), and (4) debris ejection ( $F_e$ ) (Bažant et al. 2008). In the continuum sense, these resisting forces represent the derivatives of each dissipated energy with respect to  $z$ .

The resisting force  $F_b$  due to plastic-hinge buckling and fracture of columns can be expressed by

$$F_b = \frac{\beta}{h} \int_0^{u_f} F(u) du \quad (3)$$

where  $h =$  story height;  $F(u) =$  axial force resultant of all the columns in the story as a function of the vertical relative displacement;  $u =$  relative displacement between column ends;  $u_f =$  final value of  $u$  when the story is fully crushed; and  $\beta =$  constant less than 1 but probably close to 1. Function  $F(u)$  from a three-hinge buckling mechanism [Fig. 5 in Bažant and Zhou (2002)] is given by Eq. (6) in Bažant et al. (2008). Constant  $\beta$  is introduced to account for the fact that the actual energy dissipation of column failure may be less than that calculated from an ideal three-hinge buckling mode due to three effects (Bažant et al. 2008; Le and Bažant 2017b): (1) instances of multistory buckling, (2) softening due to local plastic flange buckling, and (3) fracture of steel in inelastic hinges.

The resisting force  $F_s$  due to the comminution of concrete slabs can be calculated from the total energy expended to create all new surfaces of concrete fragments, i.e., as follows:

$$F_s = \frac{1}{h} \int_{D_{\min}}^{D_{\max}} \frac{3G_f}{\rho_c D} dm(D) \quad (4)$$

where  $D_{\max}$  and  $D_{\min} =$  maximum and minimum fragment sizes, respectively;  $G_f =$  fracture energy;  $\rho_c =$  mass density of concrete; and  $m(D) =$  mass of all fragments whose sizes are less than  $D$ . The mass distribution of the fragments is described using Schuhmann's law (Schuhmann 1940; Charles 1957)

$$m(D) = m_c (D/D_{\max})^k$$

where  $m_c =$  total mass of the concrete slab; and  $k =$  constant with typical value  $k = 1/2$ . To complete the model for  $F_s$ , it was noted that the maximum particle size  $D_{\max}$  depends on the specific impact energy:  $D_{\max} = A(0.5\dot{z}^2)^{-p}$ . Constants  $A$  and  $p$  were determined based on the observed minimum fragment size and the estimated ratio between the maximum and minimum fragment sizes [Bažant et al. (2008) has given more details].

To calculate the resisting force  $F_a$  due to air ejection, the average ejection velocity  $v_a$  was first estimated from mass conservation,

i.e.,  $\psi\rho_a V_a = \rho_a A_w v_a \Delta t_s$ , where  $\psi$  is the vent ratio (ratio of unobstructed area of the perimeter walls to their total area),  $\rho_a = 1.225 \text{ kg/m}^3$  is the air density at atmospheric pressure and room temperature,  $V_a$  is the initial volume of the air in the story, which is  $a^2 h_c$  (where  $a$  is the width of the side of square cross section of tower and  $h_c$  is the clear height of one story),  $A_w$  is the area of perimeter wall, which equals  $4ah_c$ , and  $\Delta t_s \approx h_c/\dot{z}$  is the time during which the top slab of a story collapses onto the underlying slab and thus pushes out all the air ( $\Delta t_s$  was only about 0.07 s for the lowest stories). From the average ejection velocity, we can calculate the equivalent resisting force by

$$F_a = \frac{\rho_a V_a v_a^2}{2h} = \frac{\rho_a a^4}{32\psi^2 h_c h} \dot{z}^2 \quad (5)$$

The resisting force  $F_e$  was calculated from the kinetic energy of the debris ejection. The fact that different types of debris were ejected at different velocities greatly complicates the calculation. Nevertheless, for the purpose of calculating the total kinetic energy of all the debris, it is reasonable to assume that, among all the ejected debris, a certain fraction, characterized by empirical parameter  $\kappa_e$ , gets ejected in any direction at velocity  $\dot{z}$ , whereas the rest of the debris is shed at nearly zero velocity. For a certain value of  $\kappa_e$ , this simplified calculation will give the same total kinetic energy of the ejected debris as that calculated by considering the actual distribution of velocities of different debris. Based on this simplification, as the crush front propagates by a distance of  $\delta z$ , the total kinetic energy of the ejected debris is  $\kappa_e \kappa_o \mu(z) \delta z (\dot{z}^2/2)$ . Therefore, the energy-equivalent resisting force can be expressed by

$$F_e = \frac{1}{2} \kappa_e \kappa_o \mu(z) \dot{z}^2 \quad (6)$$

Note that  $F_e$  becomes zero in the crush-up phase because the compacted layer is stationary.

It has been shown that, among the aforementioned four energy dissipation mechanisms, the buckling and fracture of steel columns play a dominant role for the entire crush-down phase (Bažant et al. 2008). Near the end of the crush-down phase,  $F_b$  was about three times the sum of  $F_e$ ,  $F_a$ , and  $F_s$ . For a brief period at the beginning of the crush-up phase, the contributions of  $F_a$  and  $F_s$

were significant but were soon overridden by  $F_b$ . Toward the end of the crush-up phase,  $F_b$  was about twice the sum of  $F_a$  and  $F_s$ . Although the contributions of  $F_s$ ,  $F_a$ , and  $F_e$  to the total energy dissipation were minor compared with that of  $F_b$ , it is essential to take them into account to explain and interpret some important observations of the tower collapse.

### Comparison with Observations

The aforementioned differential equations [Eqs. (1) and (2)] of the collapse motion can be accurately solved using the fourth-order Runge-Kutta method. The values of the model parameters have been given by Bažant et al. (2008) and Le and Bažant (2017a). The solutions of Eqs. (1) and (2) yield the complete motion history of the crush front, the collapse duration, and the size distribution of the concrete fragments.

Fig. 3 compares the motion of the topmost rim corners of the North and South Towers during the first few seconds as predicted by the model with that obtained from the available video record. The model is seen to agree with the video record quite well. Due to the larger initial falling mass, the crush front in the South Tower hit the underlying floor with a higher kinetic energy than in the North Tower. An important observation is that for both towers, the motion of the upper falling part was considerably slower than the free-fall motion, which was mainly due to the resistance of columns. One of the main points raised by the critics, claiming controlled demolition, was that the tower was in free fall, which is clearly disapproved by the video record.

Fig. 4 shows the calculated motion history of the tower during the entire collapse process. The model predicts that the crush-down phases of the North and South Towers lasted for 12.40 and 10.21 s, respectively. The actual duration of the crush-down phase has been inferred from the seismic record registered at Lamont-Doherty Earth Observatory of Columbia University. The analysis of the time history of the short-period Rayleigh surface waves showed that the crush-down durations of the North and South Towers were about 12.59 and 10.09 s, respectively (Bažant et al. 2008). As seen, the model prediction agrees well with the results obtained from the seismic record. Again, it is worth pointing out that the crush-down durations of the North and South Towers were about 65.5% and 47.3%

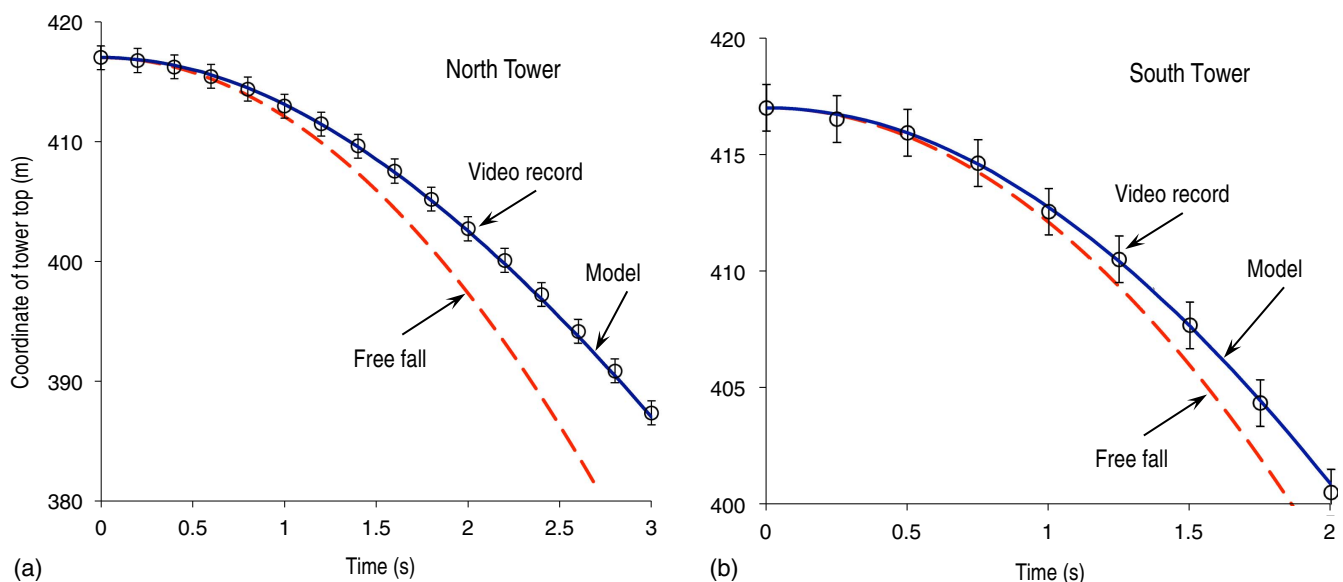


Fig. 3. Time histories of the motion of tower tops and comparison with the video record: (a) North Tower; and (b) South Tower.

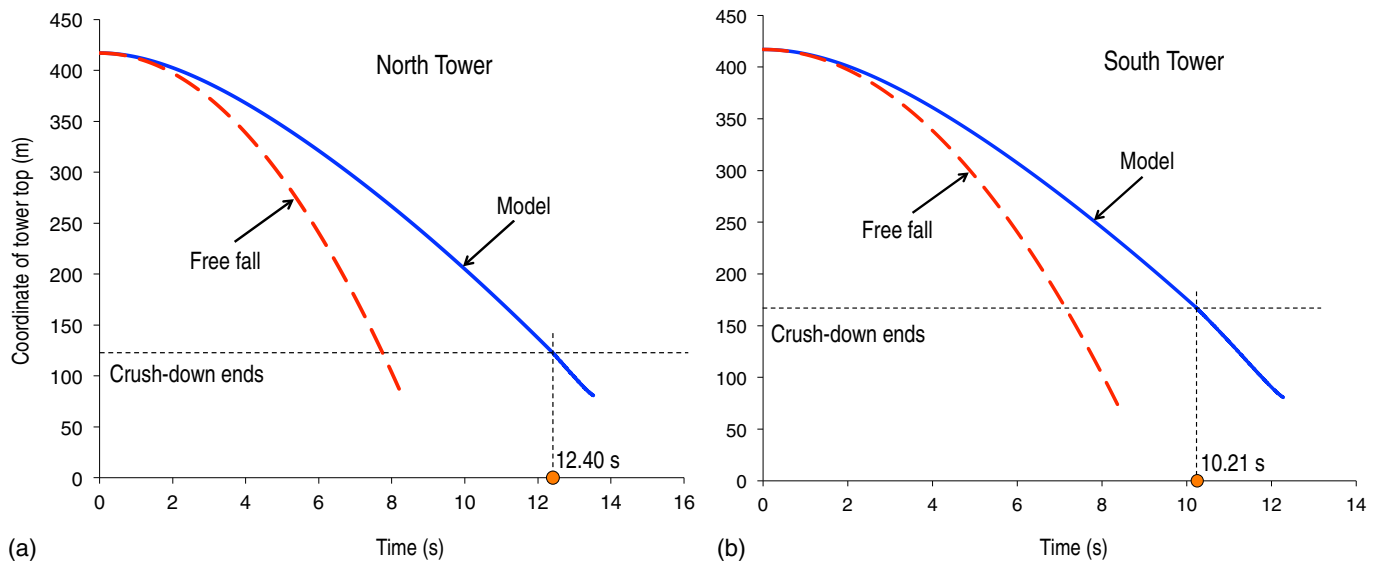


Fig. 4. Motion histories of the towers for the entire collapse duration: (a) North Tower; and (b) South Tower.

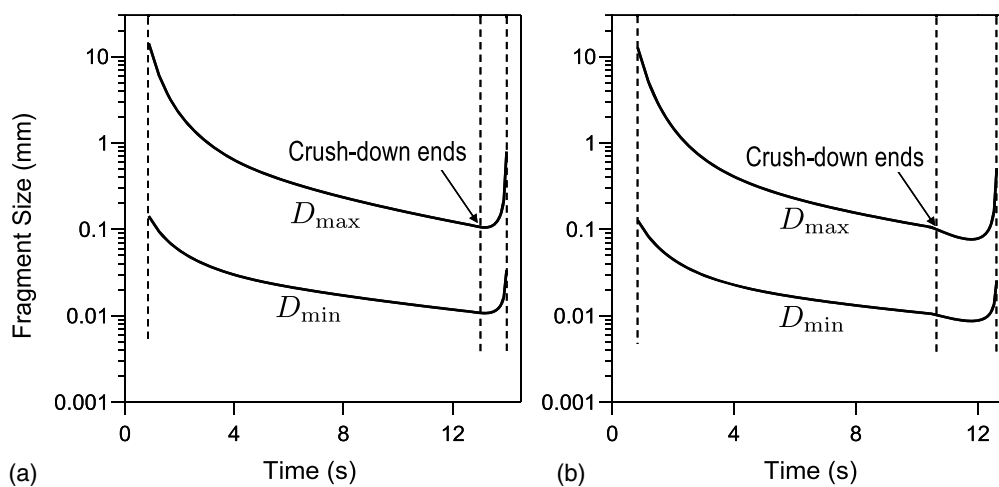


Fig. 5. Evolution of the fragment sizes at the crush front: (a) North Tower; and (b) South Tower.

longer than those of a free fall of the upper part of each tower. This clearly dispels the false claim of the control demolition proponents.

Fig. 5 presents the evolution of the maximum and minimum fragment sizes ( $D_{\max}$  and  $D_{\min}$ ) formed at the crush front. At the beginning stage of the collapse,  $D_{\max}$  was about 14 mm, and  $D_{\min}$  was about 0.14 mm. As the crush front accelerated, both  $D_{\max}$  and  $D_{\min}$  decreased significantly. The decrease in  $D_{\max}$  was more pronounced than that in  $D_{\min}$ . This is because it is much harder to fragment small particles than large particles. At the end of crush-down phase,  $D_{\max}$  was about 0.1 mm, and  $D_{\min}$  was about 10  $\mu\text{m}$ , which agrees with the size range of concrete fragments observed on the ground. It was shown that at the end of the crush-down phase, the kinetic energy of the upper falling part was far higher than that required to pulverize all the concrete slabs into particles of a size range of 10–100  $\mu\text{m}$  (Bažant et al. 2008).

The model also predicts extreme air ejection speed during the collapse process. Toward the end of the crush-down phase, this speed was on the order of 804 km/h (500 mi/h) which would create sonic booms. This also explains why large amounts of fragments and dust were ejected to a distance of several hundred meters from the tower perimeter.

## Stochastic Computational Model for RC Structures

In the aftermath of the WTC collapse, a concerted effort was directed toward developing methodologies for assessment of the vulnerability of buildings against progressive collapse. One widely adopted approach is the alternate load path analysis (ALPA) developed by the General Services Administration (GSA) (GSA 2003; DOD 2016; Ellingwood 2006; McKay et al. 2012). Its essential aspect is to investigate the behavior of the structure once a local damage occurs (usually in the form of removal of vertical load-carrying structural components). Within the framework of ALPA, a probabilistic approach has been proposed to evaluate the building vulnerability (Ellingwood 2006). The collapse probability  $P[C]$  of the structure can be calculated by

$$P[C] = \sum_H P[C|LD]P[LD|H]P[H] \quad (7)$$

where  $P[H]$  = occurrence probability of hazard  $H$ ;  $P[LD|H]$  = probability of local structural damage LD if hazard  $H$  occurs; and  $P[C|LD]$  = probability of structure collapse if local structural damage LD occurs. Among these probabilities,  $P[H]$  can be

estimated from the annual occurrence rate of the hazard (Ellingwood et al. 2007), and  $P[LD|H]$  can be conservatively taken as unity. The main challenge is the computation of  $P[C|LD]$ , which requires stochastic simulations of the nonlinear response of structural systems. In this section, we review a two-scale computational model that was recently developed for stochastic analysis of progressive collapse of RC buildings (Le and Xue 2014; Xue and Le 2016c, b).

### Model Description

The formulation of the two-scale model was motivated by the concept of cohesive fracture. In the model, we first identify the potential damage zones (PDZs) that could possibly form in various structural members. Fig. 6 shows the typical locations of PDZs in beams, columns, walls, and slabs. The size of the PDZ can be determined based on experimental observations (Aycardi et al. 1994; Panagiotou et al. 2012). Because damage can occur only in the PDZs and the materials outside these zones are considered to be elastic, the failure behavior of the structure is solely governed by the behavior of the PDZs.

In recent studies (Le and Xue 2014; Xue and Le 2016c), the PDZs were modeled by a set of cohesive elements. To formulate the cohesive law, each PDZ was separated into two parts: (1) concrete section including the transverse reinforcement (if any), and (2) longitudinal reinforcement (Fig. 7). The traction-separation relationship can then be written

$$\sigma_n = \sigma_n^c(w_n, w_m, w_l) + \rho_s \sigma_n^s(w_n, w_m, w_l) \quad (8)$$

$$\tau_m = \tau_m^c(w_n, w_m, w_l) + \rho_s \tau_m^s(w_n, w_m, w_l) \quad (9)$$

$$\tau_l = \tau_l^c(w_n, w_m, w_l) + \rho_s \tau_l^s(w_n, w_m, w_l) \quad (10)$$

where  $\sigma_n$ ,  $\tau_m$ , and  $\tau_l$  = total tractions in the normal and two orthogonal shear directions;  $\sigma_n^c$ ,  $\tau_m^c$ , and  $\tau_l^c$  = normal and shear tractions of the concrete cross section;  $\sigma_n^s$ ,  $\tau_m^s$ , and  $\tau_l^s$  = normal and shear tractions of the longitudinal reinforcement;  $w_n$ ,  $w_m$ , and  $w_l$  = normal and shear separations; and  $\rho_s$  = longitudinal reinforcement ratio.

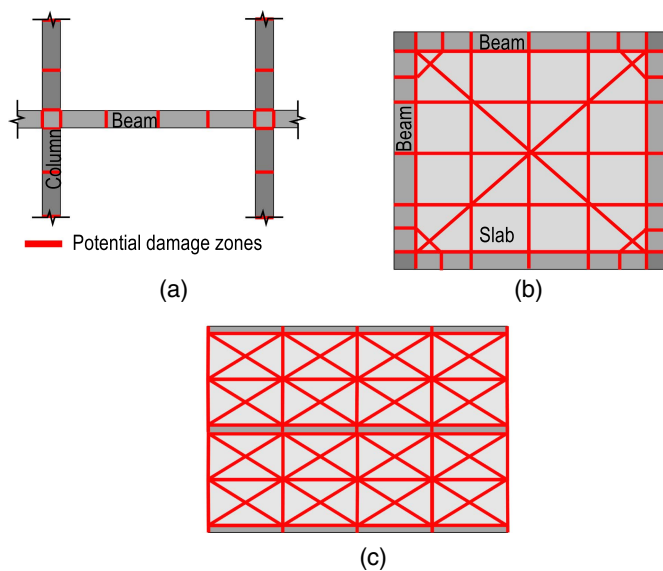


**Fig. 6.** Typical locations of the PDZ in different structural components: (a) beam and column; (b) slab; and (c) wall.

The constitutive behavior of the concrete cross section is described in terms of the effective traction-separation relationship, where the effective separation is defined by  $\bar{w} = [w_n^2 + \alpha_t^2(w_m^2 + w_l^2)]^{1/2}$ , and the effective traction  $\bar{\sigma}$  is work-conjugate to  $\bar{w}$ , where  $\alpha_i$  ( $i = t, c$ ) are constants corresponding to tension-shear and compression-shear loading modes, respectively. To capture the effect of different loading modes, the  $\bar{\sigma}$ - $\bar{w}$  relationship is made to depend on the mode mixity angle  $\theta = \tan^{-1}(w_n/\alpha_i\sqrt{w_m^2 + w_l^2})$ . Based on the work conjugacy, the normal and shear tractions ( $\sigma_n^c$ ,  $\tau_m^c$ , and  $\tau_l^c$ ) are calculated directly from the effective traction  $\bar{\sigma}$  (Le and Xue 2014).

The process of progressive collapse involves the failure of many PDZs. For the purpose of simulation of the overall collapse pattern, the detailed form of the  $\bar{\sigma}$ - $\bar{w}$  relationship is not essential. What matters is the peak load resistance and the total energy dissipation capacity of the cohesive element. It has been shown that it suffices to assume a linear softening cohesive behavior for the concrete cross section, and the cohesive strength and total energy dissipation can be obtained from the finite-element (FE) simulations of the concrete cross section of the PDZ under different loading conditions, such as uniaxial tension and compression, combined tension-shear, and combined compression-shear (Le and Xue 2014; Xue and Le 2016c, b).

In the FE simulations, nonlinear constitutive models of concrete and steel reinforcement were used. The mesh size was set to be equal to the crack band width of concrete material, and the transverse reinforcement was modeled by truss elements. The advantage of this two-scale approach is that the resulting cohesive law accounts for the behavior of the finite-size PDZ while it also captures the essential length scale of concrete fracture. The traction-separation relationship ( $\sigma_n^s$ ,  $\tau_m^s$ , and  $\tau_l^s$ ) of the longitudinal reinforcement can be derived directly from the uniaxial stress-strain relationship of the steel modified by the bond-slip effect [Lew et al. (2011), Le and Xue (2014), and Xue and Le (2016c) have given details].

The two-scale model was applied to stochastic analysis (Le and Xue 2014; Xue and Le 2016c). In this analysis, the constitutive properties of concrete, such as the tensile and compressive strengths and the fracture energy, were considered to exhibit some spatial randomness. For the steel reinforcement, the yield strength and strain, and ultimate strength and strain, were treated as random variables. With these random variables, stochastic FE simulations were performed for each PDZ under different loading modes, from which the randomness of the model parameters of the corresponding cohesive element were determined (Le and Xue 2014; Xue and Le 2016c). The resulting random cohesive parameters of the PDZs were then used for stochastic simulations of the collapse behavior of the entire structure.

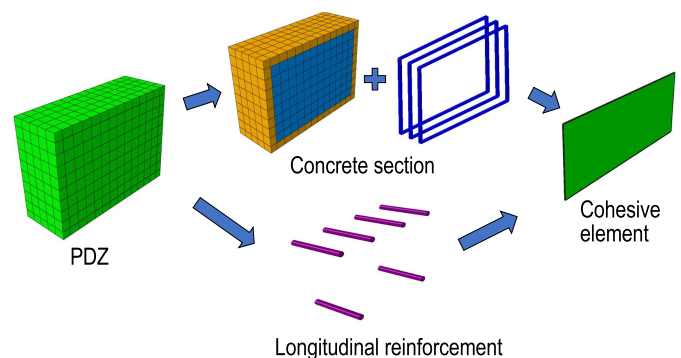


**Fig. 7.** Schematic of concept of two-scale model.

To model the progressive collapse, the cohesive element was deleted once it loses the load-carrying capacity. The deletion of cohesive elements may lead to the disintegration of the structural components, which may fall and impact the intact parts of the structure. This debris impact process was modeled by using the default contact algorithm in ABAQUS version 6.11, in which a hard contact law was used in the normal direction to minimize the overclosure, and a friction contact law was used in the tangential direction, with a friction coefficient of 0.3.

### Numerical Examples

The two-scale model was first applied to simulate a full scale push-down experiment on a RC structural subassembly (Lew et al. 2011; Sadek et al. 2011) [Fig. 8(a)]. The test was performed under a displacement controlled mode to resemble a column removal scenario. In the numerical study, this push-down test was simulated by the two-scale model and also by a detailed FE model (Xue and Le 2016a).

In the FE model, the concrete was modeled by continuum elements, and the steel reinforcement was modeled by truss elements. A damage plasticity model was used to describe the constitutive behavior of concrete, and an isotropic kinematic hardening model was used for steel reinforcement. The material properties have been given by Lew et al. (2011) and Sadek et al. (2011). The size of the finite-element mesh was set to be equal to the crack band width.

In the two-scale model, the cohesive properties of the PDZs were first determined by performing FE simulations of the PDZs

under different loading conditions. The calibrated cohesive model was then used to simulate the behavior of the subassembly. Fig. 8(b) shows the measured and simulated load-displacement curves at the center of the subassembly. The two-scale model agreed well with the experimental result as well as the simulation by the FE model. In particular, the model could capture quite well the overall load capacity and the energy dissipation capacity of the structure. Furthermore, the model also predicted well different nonlinear behaviors of the structure, such as the arching effect of the frame, damage of concrete material, catenary action, and tensile rupture of the longitudinal reinforcement (Sadek et al. 2011; Le and Xue 2014). The agreement between the two-scale model and the FE model verifies the concept of the two-scale representation of the structural behavior and the calibration procedure for the cohesive elements.

In the second example, the two-scale model was used to investigate the stochastic response of a prototype 10-story RC building. The design of the building has been given by Bao et al. (2008) and Bao and Kunnath (2010) (Fig. 9). The study considered four local-damage scenarios, which included the removal of two adjacent corner columns (Grids F-5 and F-6) on Stories 1, 5, 9, and 10, respectively. In the stochastic simulation, both random material properties and gravity loads were considered. A gravity load combination of  $1.05 \text{ DL} + 0.3 \text{ LL}$  was used (where DL is the nominal dead load and LL is the nominal live load) (Xu and Ellingwood 2011). The details of the probability distributions of gravity loads can be found in Xue and Le (2016c). The simulation predicts the occurrence probabilities of collapse of different extents. In addition,

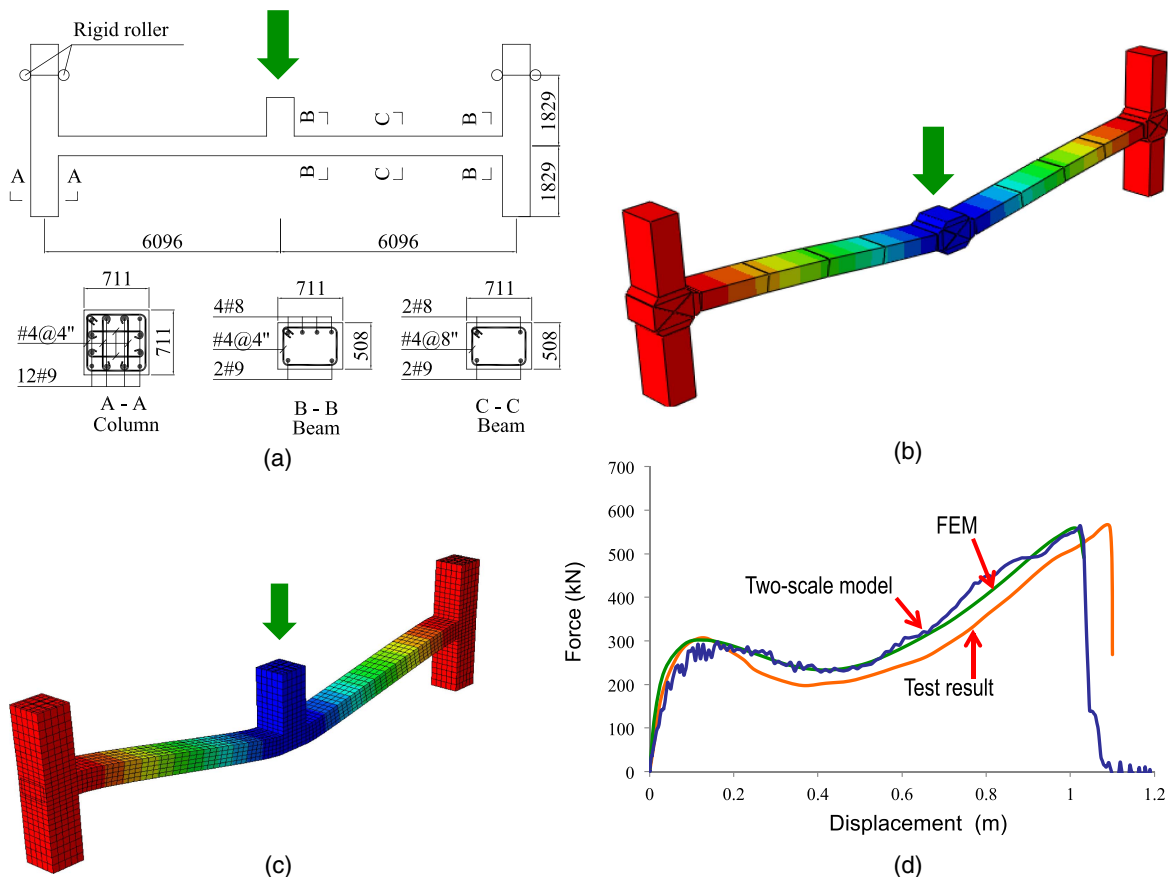


**Fig. 8.** Simulation of NIST push-down experiment: (a) design of frame subassembly; (b) two-scale model; (c) FE model; and (d) comparison of the measured and simulated load-deflection curves.

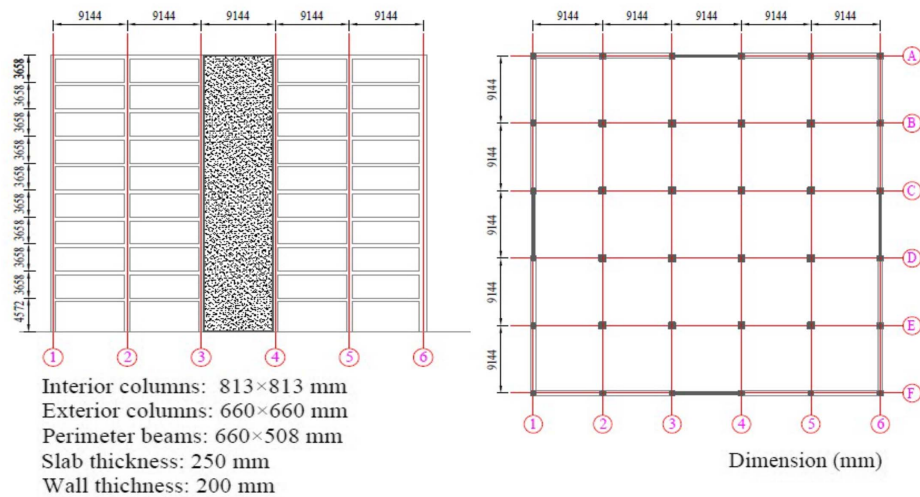


**Fig. 9.** Design of 10-story prototype building [reproduced from Xue and Le (2016c)].

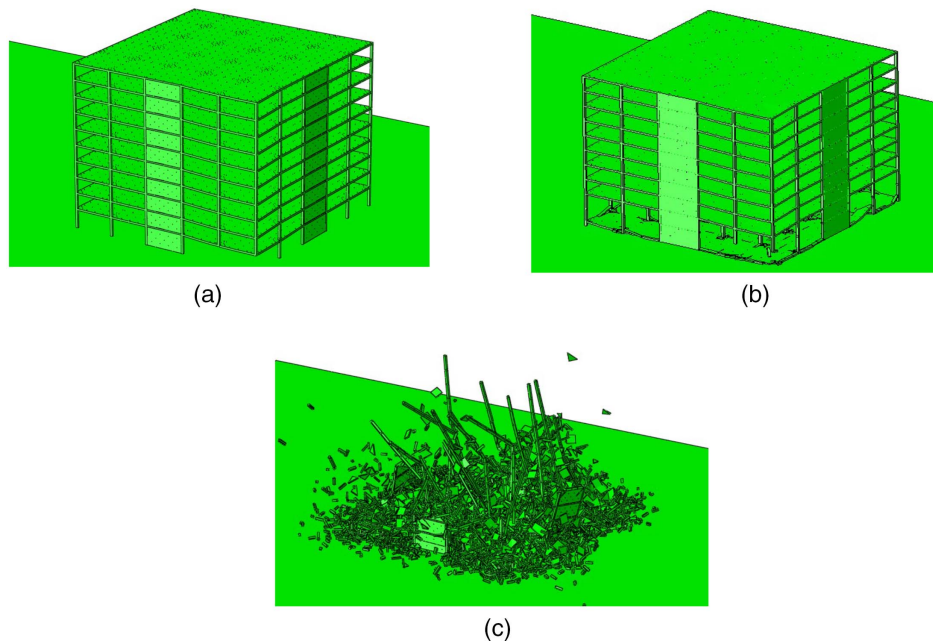


**Fig. 10.** Different simulated collapse extents: (a) intact; (b) partial collapse; and (c) total collapse [reproduced from Xue and Le (2016c)].

conventional mean-centered deterministic simulations, which use the mean material properties and a combination of mean gravity loads  $1.2 \text{ DL} + 0.5 \text{ LL}$  (DOD 2016; Xu and Ellingwood 2011), were also performed. The building was assumed to have a 5% damping ratio.

The simulation shows that the model was able to capture both the crush-up and crush-down phases of the collapse process. The stochastic analysis captured different possible failure paths caused by the randomness of material properties and applied gravity loads. On the contrary, the deterministic calculation only captured the dominant failure path that corresponds to the mean behavior. This caused some differences in the prediction of the effect of initial damage location on the overall collapse resistance (Xue and Le 2016c).

Based on the simulation results, collapses of three extents (intact structure, partial collapse, and total collapse) were identified

(Fig. 10). The intact condition means that initial local damage does not propagate. The partial collapse refers to the case in which the initial damage propagates with only a limited damage spread defined by (1) horizontal damage spreading to less than 25% of the floor plan if the vertical damage spreads more than one floor, or (2) the vertical damage spreading one floor only. The total collapse refers to the case where the damage spreads beyond the extent of partial collapse.

Table 1 presents the results of the stochastic and deterministic analyses. The comparison of these results reveals the implication of the UFC load factors for the collapse risk of the building. The total collapse probability of a general building should be limited to the order of  $10^{-6}$ , and the occurrence probability of a local damage scenario due to hazards is on the order of  $10^{-4}$  (Ellingwood 2006). Therefore, the tolerable collapse probability for a given local damage scenario should be on the order of 0.01. Based on Table 1, the

**Table 1.** Occurrence probabilities of collapse extents

Location of column removal	Stochastic analysis			Collapse extent predicted by deterministic analysis
	Intact	Partial	Total	
1st story	0.2450	0.0600	0.6950	Total
5th story	0.4650	0.0000	0.5350	Total
9th story	0.9233	0.0000	0.0767	Total
10th story	0.9950	0.0000	0.0050	Intact

mean-centered deterministic analysis was able to predict the collapse with an actual occurrence probability around 7.67% for a given local damage scenario, which is sufficient for most buildings. However, it does not predict a collapse event with an occurrence probability of 0.5%, which could still be of interest if a more stringent risk level is required for the building. In such a case, a probabilistic analysis is needed.

The present analysis shows that, except for the case of column removal at the first floor, the building would suffer total collapse once the initially damaged floor collapses. Therefore, for practical purposes, the vulnerability of the structure against progressive collapse can be assessed by investigating the behavior of the initially damaged floor. This result is consistent with the finding of the previous research, which suggested considering the failure of a single floor as the robustness limit state (Izzuddin et al. 2008; DOD 2016).

### Delayed Collapse of RC Frames

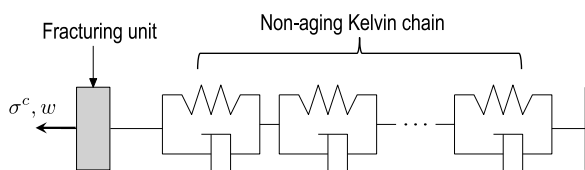
A recent experiment on the progressive collapse of a 3-story, 3 bay  $\times$  3 bay RC frame showed that the structure could exhibit a delayed collapse (Xiao et al. 2015). It was speculated that this delayed collapse can be attributed to time-dependent behavior of the concrete material (Xiao et al. 2015). Motivated by this experiment, the two-scale model presented in the previous section was recently extended to the modeling of time-dependent collapse of RC frames (Mello et al. 2020).

In this extended model, the cohesive behavior of the concrete section of the PDZs was modeled by coupling a cohesive fracture unit with a nonaging Kelvin chain (Fig. 11). The Kelvin chain is used to describe the viscoelastic response of concrete. The compliance function was approximated by the Dirichlet series (Bažant and Jirásek 2018) [Mello et al. (2020) has given a detailed formulation]. The part of the structure outside the PDZs was modeled by standard continuum elements. Although these elements do not experience damage, they share the same viscoelastic behavior as the PDZs.

The cohesive fracture unit features a damage growth model that captures the subcritical damage growth mechanism of concrete. The effective traction-separation relation is expressed in the framework of damage mechanics

$$\bar{\sigma} = (1 - \omega)C\bar{w}_f \quad (11)$$

where  $\omega$  = damage parameter ranging from 0 (virgin state) to 1 (fully damaged state);  $\bar{w}_f$  = effective separation of the fracturing

**Fig. 11.** Time-dependent cohesive model of PDZ.

unit; and  $C$  = elastic stiffness. The subcritical damage growth is described by the following kinetic model:

$$\frac{d\omega}{dt} = \frac{B\lambda^k}{(1 - \omega)^r} \quad (12)$$

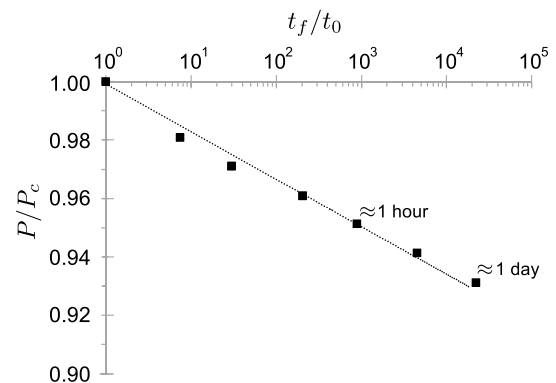
where  $\lambda = \bar{\sigma}/\sigma_p$ , where  $\sigma_p$  is peak load resistance of the fracturing unit; and  $B$ ,  $k$ , and  $r$  = constants. Eqs. (11) and (12) predict the loading path in the traction-separation space. The modeled loading path is bounded by a bilinear traction-separation envelope, which represents the behavior of the fracturing unit under monotonic fast loading.

The model was applied to simulate the delayed collapse behavior of the aforementioned NIST frame subassembly [Fig. 8(a)]. In the simulation, the applied displacement was increased monotonically until the load reached a prescribed level  $P$ , which was lower than the first peak load  $P_c$  measured in the push-down experiment. The applied load was then held constant all the way until failure. The failure was largely due to the time-dependent damage accumulation and load-redistribution mechanism. The key output is the time to failure  $t_f$ , which is usually referred to as the structural lifetime. Because the interest of time scale for studying the delayed collapse behavior is on the order of a few days at maximum, the simulation focused on the high load levels, i.e.,  $P/P_c \geq 0.93$ .

Fig. 12 shows the simulated relationship between the sustained loading level  $P/P_c$  and the structural lifetime. It is seen that the relation follows an inverse power law, which is consistent with the results of experimental and numerical studies on the creep-rupture behavior of concrete specimens (Boumakisa et al. 2018; Di Luzio 2009). For  $P/P_c = 93\%$ , the subassembly would fail in a day.

The aforementioned simulation result has important implications for the analysis of progressive collapse. After the sudden removal of columns or walls, the adjacent structural members would experience some damage, but the damage may not be severe enough to cause incipient collapse. The existing APLA approach would consider the structure to be safe because no instantaneous collapse occurred.

The present model, however, raises a new consideration. Although the structural members may not fail immediately after the sudden removal of columns or walls, they could experience some level of damage, and the damage could continuously grow under the increased gravity loading due to the column or wall removal. Over time, the loading-carrying capacity of the structure member could decrease to a level that is lower than the sustained gravity load, and dynamic failure would happen. This could trigger the collapse of the entire structural system. Depending on the predamage

**Fig. 12.** Simulated load-lifetime curve ( $t_0$  = time to reach the peak load in the simulation of  $P = P_c$ ).

level caused by the column removal as well as the gravity load level after column removal, the time scale of delayed collapse could be on the order of several hours or a day, which is within the time frame of occupant evacuation and operation of first responders.

## Summary and Conclusions

Based on the analyses conducted and the results obtained, the following conclusions can be reported:

- Progressive collapse of building systems is a complex physical process that involves different nonlinear phenomena such as material damage and fracture, fragmentation, and debris impact. Despite this complexity, tractable analytical and computational models can be formulated to simulate the collapse behavior.
- The 1D mathematical modeling of the collapse of WTC towers captured the essential energy dissipation mechanisms of the collapse. The simulation agreed well with different observations of the collapse process including the tower motion, collapse duration, fragment size distribution, and ejection of air and debris, with loud booms. The numerical calculations proved that the total collapse of the towers that was triggered, about 1 h after aircraft impact by a long-lasting fire engulfing simultaneously several entire stories, was spontaneous.
- To model the probabilistic collapse behavior of RC frame structures, a two-scale computational model was developed. The model successfully captured the effects of random material properties and gravity loads on the occurrences of collapse of different extent. The simulation results showed that the existing mean-centered deterministic analysis was able to guarantee a tolerable collapse risk of a level acceptable for conventional buildings. For sensitive structures with a more stringent requirement on the tolerable risk, a detailed stochastic analysis would be needed.
- The latest extension of the two-scale model to time-dependent progressive collapse showed that the structure may remain standing after local structural damage but collapse later. The damage accumulation and viscoelastic deformation of concrete are the mechanisms that may lead to a delayed structural failure. Understanding of the delayed collapse behavior requires a new approach to the assessment of the collapse vulnerability of buildings and structures.

## Data Availability Statement

The computer code and simulation data generated from the study are available from the corresponding author by request.

## Acknowledgments

J.-L. Le acknowledges partial financial support from the Nuclear Engineering University Program of the Department of Energy under Grant DE-NE0008785 to the University of Minnesota. Z. P. Bažant acknowledges partial financial support under NSF Grant CMMI-2029641 to Northwestern University.

## References

Abboud, N., M. Levy, D. Tennant, J. Mould, H. Levine, S. King, C. Ekwueme, A. Jain, and G. Hart. 2003. "Anatomy of a disaster: A structural investigation of the World Trade Center collapses." In *Proc., 3rd Forensic Engineering Congress*, 360–370. Reston, VA: ASCE.

- Alashker, Y., H. Li, and S. El-Tawil. 2011. "Approximations in progressive collapse modeling." *J. Struct. Eng.* 137 (9): 912–924.
- Aycardi, L. E., J. B. Mander, and A. M. Reinfort. 1994. "Seismic resistance of reinforced concrete frame structures designed only for gravity loads: Experimental performance of subassemblages." *ACI Struct. J.* 91 (5): 552–563.
- Bao, Y., and S. K. Kunnath. 2010. "Simplified progressive collapse simulation of RC frame-wall structures." *Eng. Struct.* 32 (10): 3153–3162. <https://doi.org/10.1016/j.engstruct.2010.06.003>.
- Bao, Y., S. K. Kunnath, S. El-Tawil, and H. S. Lew. 2008. "Macromodel-based simulation of progressive collapse: RC frame structures." *J. Struct. Eng.* 134 (7): 1079–1091. [https://doi.org/10.1061/\(ASCE\)0733-9445\(2008\)134:7\(1079\)](https://doi.org/10.1061/(ASCE)0733-9445(2008)134:7(1079)).
- Bažant, Z. P. 2001. "Why did the World Trade Center collapse?" *SIAM J. Math. Anal.* 34 (8): 1–3.
- Bažant, Z. P., and M. Jirásek. 2018. *Creep and hygrothermal effects in concrete structures*. Berlin: Springer.
- Bažant, Z. P., J.-L. Le, F. R. Greening, and D. Benson. 2008. "What did and did not cause collapse of WTC Twin Towers in New York." *J. Eng. Mech.* 134 (10): 892–906. [https://doi.org/10.1061/\(ASCE\)0733-9399\(2008\)134:10\(892\)](https://doi.org/10.1061/(ASCE)0733-9399(2008)134:10(892)).
- Bažant, Z. P., and M. Verdure. 2007. "Mechanics of progressive collapse: Learning from World Trade Center and building demolitions." *J. Eng. Mech.* 133 (3): 308–319. [https://doi.org/10.1061/\(ASCE\)0733-9399\(2007\)133:3\(308\)](https://doi.org/10.1061/(ASCE)0733-9399(2007)133:3(308)).
- Bažant, Z. P., and Y. Zhou. 2002. "Why did the World Trade Center collapse?—Simple analysis." *J. Eng. Mech.* 128 (1): 2–6. [https://doi.org/10.1061/\(ASCE\)0733-9399\(2002\)128:1\(2\)](https://doi.org/10.1061/(ASCE)0733-9399(2002)128:1(2)).
- Boumakisa, I., G. Di Luzio, M. Marcon, J. Vorel, and R. Wan-Wendner. 2018. "Discrete element framework for modeling tertiary creep of concrete in tension and compression." *Eng. Frac. Mech.* 200 (Sep): 263–282.
- Charles, R. J. 1957. "Energy-size reduction relationships in comminution." *Min. Eng.* 9 (14): 80–88.
- Di Luzio, G. 2009. "Numerical model for time-dependent fracturing of concrete." *J. Eng. Mech.* 135 (7): 632–640. [https://doi.org/10.1061/\(ASCE\)0733-9399\(2009\)135:7\(632\)](https://doi.org/10.1061/(ASCE)0733-9399(2009)135:7(632)).
- DOD (Department of Defense). 2016. *Design of buildings to resist progressive collapse, with change 3*. Washington, DC: DOD.
- Ellingwood, B. R. 2006. "Mitigating risk from abnormal loads and progressive collapse." *J. Perform. Constr. Facil.* 20 (4): 315–323. [https://doi.org/10.1061/\(ASCE\)0887-3828\(2006\)20:4\(315\)](https://doi.org/10.1061/(ASCE)0887-3828(2006)20:4(315)).
- Ellingwood, B. R., R. Smilowitz, D. O. Dusenberry, D. Duthinh, H. S. Lew, and N. J. Carino. 2007. *Best practices for reducing the potential for progressive collapse in buildings*. Gaithersburg, MD: National Institute of Standards and Technology.
- El-Tawil, S., H. Li, and S. Kunnath. 2014. "Computational simulation of gravity-induced progressive collapse of steel-frame buildings: Current trends and future research needs." *J. Struct. Eng.* 140 (8): A2513001. [https://doi.org/10.1061/\(ASCE\)ST.1943-541X.0000897](https://doi.org/10.1061/(ASCE)ST.1943-541X.0000897).
- GSA (General Services Administration). 2003. *Progressive collapse analysis and design guidelines for new federal office buildings and major modernization projects*. Washington, DC: GSA.
- Izzuddin, B. A., A. G. Vlassis, A. Y. Elghazouli, and D. A. Nethercot. 2008. "Progressive collapse of multi-storey buildings due to sudden column loss—Part I: Simplified assessment framework." *Eng. Struct.* 30 (5): 1308–1318. <https://doi.org/10.1016/j.engstruct.2007.07.011>.
- Kaewkulchai, G., and E. B. Williamson. 2004. "Beam element formulation and solution procedure for dynamic progressive collapse analysis." *Comput. Struct.* 82 (7–8): 639–651. <https://doi.org/10.1016/j.compstruc.2003.12.001>.
- Kausel, E. 2001. "Inferno at the World Trade Center." In *The towers lost and beyond*, edited by E. Kausel. Cambridge, MA: MIT Press.
- Khandelwal, K., and S. El-Tawil. 2008. "Pushdown resistance as a measure of robustness in progressive collapse analysis." *Eng. Struct.* 33 (9): 2653–2661. <https://doi.org/10.1016/j.engstruct.2011.05.013>.
- Kiaokojouri, F., V. D. Biagi, B. Chiaia, and M. R. Sheidaii. 2020. "Progressive collapse of framed building structures: Current knowledge and future prospects." *Eng. Struct.* 206 (Jan): 110061.

- Le, J.-L., and Z. P. Bažant. 2011. "Why the observed motion history of World Trade Center towers is smooth." *J. Eng. Mech.* 137 (1): 82–84. [https://doi.org/10.1061/\(ASCE\)EM.1943-7889.0000198](https://doi.org/10.1061/(ASCE)EM.1943-7889.0000198).
- Le, J.-L., and Z. P. Bažant. 2017a. "Mechanics-based mathematical studies proving spontaneity of post-impact WTC towers collapse." *Europhys. News* 48 (1): 18–23. <https://doi.org/10.1051/eprn/2017102>.
- Le, J.-L., and Z. P. Bažant. 2017b. "Mechanics of collapse of WTC towers clarified by recent column buckling tests of Korol and Sivakumaran." *Int. J. Struct. Stab. Dyn.* 17 (9): 1771011. <https://doi.org/10.1142/S0219455417710110>.
- Le, J.-L., and B. Xue. 2014. "Probabilistic analysis of reinforced concrete frame structures against progressive collapse." *Eng. Struct.* 76 (2): 313–323. <https://doi.org/10.1016/j.engstruct.2014.07.016>.
- Lew, H. S., Y. Bao, F. Sadek, and J. A. Main. 2011. *An experimental and computational study of reinforced concrete assemblies under a column removal scenario*. Gaithersburg, MD: National Institute of Standards and Technology.
- Masoero, E., F. K. Wittel, H. J. Herrmann, and B. M. Chiaia. 2010. "Progressive collapse mechanisms of brittle and ductile framed structures." *J. Eng. Mech.* 136 (8): 987–995. [https://doi.org/10.1061/\(ASCE\)EM.1943-7889.0000143](https://doi.org/10.1061/(ASCE)EM.1943-7889.0000143).
- McKay, A., K. Marchand, and M. Diaz. 2012. "Alternate path method in progressive collapse analysis: Variation of dynamic and nonlinear load increase factors." *Prac. Period. Struct. Des. Constr.* 17 (4): 152–160. [https://doi.org/10.1061/\(ASCE\)SC.1943-5576.0000126](https://doi.org/10.1061/(ASCE)SC.1943-5576.0000126).
- Mello, L., J.-L. Le, and R. Ballarini. 2020. "Numerical modeling of delayed progressive collapse of reinforced concrete structures." *J. Eng. Mech.* 146 (10): 04020113. [https://doi.org/10.1061/\(ASCE\)EM.1943-7889.0001843](https://doi.org/10.1061/(ASCE)EM.1943-7889.0001843).
- NIST. 2005. *Final report on the collapse of the World Trade Center towers*. Gaithersburg, MD: NIST.
- Panagiotou, M., J. Restrepo, M. Schoettler, and G. Kim. 2012. "Nonlinear cyclic truss model for reinforced concrete walls." *ACI Struct. J.* 109 (2): 205–214.
- Pesce, C. P., L. Casetta, and F. M. dos Santos. 2012. "Equation of motion governing the dynamics of vertically collapsing buildings." *J. Eng. Mech.* 138 (12): 1420–1431. [https://doi.org/10.1061/\(ASCE\)EM.1943-7889.0000453](https://doi.org/10.1061/(ASCE)EM.1943-7889.0000453).
- Quintiere, J. G., M. di Marzio, and R. Becker. 2002. "A suggested cause of the fire-induced collapse of the World Trade Towers." *Fire Saf. J.* 37 (7): 707–716. [https://doi.org/10.1016/S0379-7112\(02\)00034-6](https://doi.org/10.1016/S0379-7112(02)00034-6).
- Sadek, F., J. M. Main, H. S. Lew, and Y. Bao. 2011. "Testing and analysis of steel and concrete beam-column assemblies under a column removal scenario." *J. Struct. Eng.* 137 (9): 881–892. [https://doi.org/10.1061/\(ASCE\)ST.1943-541X.0000422](https://doi.org/10.1061/(ASCE)ST.1943-541X.0000422).
- Sasani, M., A. Kazemi, S. Sagioglu, and S. Forest. 2011. "Progressive collapse resistance of an actual 11-story structure subjected to severe initial damage." *J. Struct. Eng.* 137 (9): 893–902. [https://doi.org/10.1061/\(ASCE\)ST.1943-541X.0000418](https://doi.org/10.1061/(ASCE)ST.1943-541X.0000418).
- Sasani, M., and S. Sagioglu. 2008. "Progressive collapse resistance of Hotel San Diego." *J. Struct. Eng.* 134 (3): 478–488. [https://doi.org/10.1061/\(ASCE\)0733-9445\(2008\)134:3\(478\)](https://doi.org/10.1061/(ASCE)0733-9445(2008)134:3(478)).
- Schuhmann, R. 1940. *Principles of comminution. I: Size distribution and surface calculation*. New York: American Institute of Mining, Metallurgical, and Petroleum Engineers.
- Song, B. I., and H. Sezen. 2013. "Experimental and analytical progressive collapse assessment of a steel frame building." *Eng. Struct.* 56 (Apr): 664–672. <https://doi.org/10.1016/j.engstruct.2013.05.050>.
- Wierzbicki, T., and X. Teng. 2003. "How the airplane wing cut through the exterior columns of the world trade center." *Int. J. Impact Eng.* 28 (Sep): 601–625. [https://doi.org/10.1016/S0734-743X\(02\)00106-9](https://doi.org/10.1016/S0734-743X(02)00106-9).
- Xiao, Y., S. Kunnath, F. W. Li, Y. B. Zhao, H. S. Lew, and Y. Bao. 2015. "Collapse test of a 3-story half-scale RC frame building." *ACI Struct. J.* 112 (4): 429–438.
- Xu, G., and B. R. Ellingwood. 2011. "Probabilistic robustness assessment of pre-Northridge steel moment resisting frames." *J. Struct. Eng.* 137 (9): 925–934. [https://doi.org/10.1061/\(ASCE\)ST.1943-541X.0000403](https://doi.org/10.1061/(ASCE)ST.1943-541X.0000403).
- Xue, B., and J.-L. Le. 2016a. *Risk assessment of reinforced concrete buildings against progressive collapse*. ACI SP-309, Structural Integrity and Resilience, Paper No. 309-8. Montreal: ACI.
- Xue, B., and J.-L. Le. 2016b. "Simplified energy-based analysis of collapse risk of reinforced concrete buildings." *Struct. Saf.* 63 (Apr): 47–58. <https://doi.org/10.1016/j.strusafe.2016.07.003>.
- Xue, B., and J.-L. Le. 2016c. "Stochastic computational model for progressive collapse of reinforced concrete buildings." *J. Struct. Eng.* 142 (7): 04016031. [https://doi.org/10.1061/\(ASCE\)ST.1943-541X.0001485](https://doi.org/10.1061/(ASCE)ST.1943-541X.0001485).